fractal and fractional

MDPI

Article

Detection of Gate Valve Leaks through the Analysis Fractal Characteristics of Acoustic Signal

Ayrat Zagretdinov *, Shamil Ziganshin, Eugenia Izmailova, Yuri Vankov, Ilya Klyukin and Roman Alexandrov

Industrial Heat Power and Heat Supply Systems, Kazan State Power Engineering University, 420066 Kazan, Russia

* Correspondence: zagretdinov.ar@kgeu.ru

Abstract: This paper considers the possibility of using monofractal and multifractal analysis of acoustic signals to detect water leaks through gate valves. Detrended fluctuation analysis (DFA) and multifractal detrended fluctuation analysis (MF-DFA) were used. Experimental studies were conducted on a ½-inch nominal diameter wedge valve, which was fitted to a ¾-inch nominal diameter steel pipeline. The water leak was simulated by opening the valve. The resulting leakage rates for different valve opening conditions were 5.3, 10.5, 14, 16.8, and 20 L per minute (L/min). The Hurst exponent for acoustic signals in a hermetically sealed valve is at the same level as a deterministic signal, while the width of the multifractal spectrum closely matches that of a monofractal process. When a leak occurs, turbulent flow pulsations appear, and with small leak sizes, the acoustic signals become anticorrelated with a high degree of multifractality. As the leakage increases, the Hurst exponent also increases and the width of the multifractal spectrum decreases. The main contributor to the multifractal structure of leak signals is small, noise-like fluctuations. The analysis of acoustic signals using the DFA and MF-DFA methods enables determining the extent of water leakage through a non-sealed gate valve. The results of the experimental studies are in agreement with the numerical simulations. Using the Ansys Fluent software (v. 19.2), the frequencies of flow vortices at different positions of gate valve were calculated. The k-ω SST turbulence model was employed for calculations. The calculations were conducted in a transient formulation of the problem. It was found that as the leakage decreases, the areas with a higher turbulence eddy frequency increase. An increase in the frequency of turbulent fluctuations leads to enhanced energy dissipation. Some of the energy from ordered processes is converted into the energy of disordered processes.

Keywords: fractal; hurst exponent; leak; valve; shut-off valves; DFA; MF-DFA; acoustic signal

Citation: Zagretdinov, A.; Ziganshin, S.; Izmailova, E.; Vankov, Y.; Klyukin, I.; Alexandrov, R. Detection of Gate Valve Leaks through the Analysis Fractal Characteristics of Acoustic Signal. *Fractal Fract.* **2024**, *8*, 280. https://doi.org/10.3390/fractalfract8050280

Academic Editor: Carlo Cattani

Received: 10 April 2024
Revised: 2 May 2024
Accepted: 4 May 2024
Published: 8 May 2024

1. Introduction

Shut-off valves are an important part of an automation system, as they are the final actuators in automatic control [1]. Shut-off valves play a significant role in the oil, chemical and gas processing industries [2]. Corrosion, continuous contact with the fluid being pumped, operation at elevated temperatures and pressures, and other unfavorable conditions can cause leakage of shut-off valves [2,3]. Improper operation of the valve can lead to losses, decreased energy efficiency, and compromised safety of technological processes.

Valve leaks that occur in the external environment may be detected during an external inspection through traces of frost formation, leakage, gas contamination, and noise near the valve. However, leaks within the valve assembly have no external indicators and require the use of specialized inspection methods. Such methods include hydro- or pneumatic tests with pressure measurements before and after valve closure. Such tests are time-consuming and not suitable for operational monitoring.

The acoustic leak detection technique is widely employed as an express method for verifying the tightness of valve gates [1–3].

It is based on the collection and analysis of various sound signals generated by an object when a liquid or gas is flowing through a leak.

During the flow of liquid media, low-frequency acoustic methods can be used, while for gaseous media, high-frequency methods are employed (using ultrasonic acoustic emission sensors). Leakage is usually detected by an increase in the amplitude of the acoustic signal (in spectrum processing, the harmonics amplitude).

Various methods are used to process acoustic signals. The most common of these is Fourier transform (FFT). However, this method is limited because it can only extract the frequency content of a signal, losing its temporal information [4,5]. In [6,7], the power of the acoustic emission signal calculated from the spectrum power density correlated well with factors affecting leakage rates. Other authors used the method of non-linear regression (kernel partial least-squares regression) to quantify leakage rates [8]. In article [9], Gaussian process regression was used to create a multidimensional mathematical model describing the relationship between acoustic emission characteristics and leakage rates. In article [10], a least squares coefficient was selected to connect the standard deviation with leakage and create a mathematical model for internal valve leakage.

Recently, more powerful tools have been used to analyze time-varying non-stationary signals, including wavelet analysis. This enables exploring the signal simultaneously in both the time and frequency domains. However, the results obtained strongly depend on the correct choice of the original wavelet [11].

Intensive development of machine learning algorithms has made it possible to use them for leak detection and classification. In article [12], a correlation model based on a neural network was proposed, which determines the location and rate of internal leaks with acceptable errors. In [13], a neural network capable of predicting the level of internal valve leakage in natural gas pipelines was proposed. Disadvantages of using neural networks include dependence on the choice of source data, complexity of training, need for large amounts of source data and computing resources.

The task of finding an inexpensive and simple method for monitoring the tightness of pipe fittings remains relevant. Recently, fractal theory has been widely used in practical engineering to study the laws governing various complex, irregular and chaotic processes. Fractal methods are used in industries such as medicine (for analyzing data to detect cancer cells) [14–16], finance (to determine trends in securities charts) [17], meteorology [18], engineering [19–22], and other fields [23,24]. Monofractal models cannot always provide a complete description of patterns, especially when attempting to capture subtle spatial and temporal variations that are governed by natural laws. In these cases, multifractal analysis can be useful [25]. The theory of multifractals has been successfully applied to studying the aggregation properties of blood cell elements [26], the structure of DNA molecules [27], diffusive cluster growth [28], one-dimensional random walks and Brownian motion [29], and time series analysis [30,31].

This work is devoted to the study of the possibility of using monofractal and multifractal analysis methods for acoustic leak monitoring of shut-off valves. Experimental studies were conducted on wedge gate valves, during which leaks were simulated by covering the valve. Detrended fluctuation analysis (DFA) and multifractal detrended fluctuation analysis (MF-DFA) were used.

The main findings of this study are presented below:

- With small leakage values, acoustic signals exhibit anticorrelation and a high degree of multifractal behavior. As the leakage increases, correlated dynamics emerge and the degree of multifractality decreases.
- The degree of dissipation of turbulent energy in a fluid flow influences the fractal characteristics of acoustic signals.
- The results of calculating the Hurst exponent using the DFA method are dependent on the choice of degree of the fitting polynomial. In order to control the tightness of the valve, it would be advisable to use a linear approximation.
- The analysis of acoustic signals using the DFA and MF-DFA techniques enables the determination of the magnitude of water leakage through a non-sealed gate valve.

This article has the following structure:

- Section 2 presents algorithms for the analysis of acoustic signals and a description of the experimental setup;
- Section 3 presents the findings of the analysis of acoustic signals using DFA and MF-DFA methods, the outcomes of calculating the frequency of turbulence eddy frequency in Ansys Fluent, and a comparison of DFA methods with different orders;
- In conclusion, the key findings of this study are presented.

2. Materials and Methods

2.1. The DFA Algorithm

One of the approaches to describing long-term correlations in experimental data is the detrended fluctuation analysis method. Developed by Peng K.K. et al. [32], the DFA algorithm includes the following operations:

1. The fluctuation profile of the signal is being created $x(i)$ (i = 0, 1, 2, . . ., N):

$$y(i) = \sum_{k=1}^{i}(x_k - \langle x \rangle),\ i = 1, \ldots,\ N, \tag{1}$$

where $\langle x \rangle$—average value for the series.

2. The profile $y(i)$ is divided into $N_s = (N/s)$ segments of the same length s.
3. The local trend of $y(i)$ is approximated by a polynomial of $y_v(i)$ within each segment, and the variance is determined for each segment v = 1, . . ., N_s:

$$F^2(v,s) = \frac{1}{s}\sum_{i=1}^{s}[y((v-1)s+i) - y_v(i)]^2, \tag{2}$$

The DFA-1 method involves subtracting a linear trend, the DFA-2 method involves quadratic, and the DFA-3 method involves cubic, etc.

4. The resulting fluctuation function is calculated by averaging over all windows v:

$$F(s) = \left\{\frac{1}{N_s}\sum_{v=1}^{N_s} F^2(v,s)\right\}^{1/2}, \tag{3}$$

5. To determine the dependence of the log $F(s)$ on the log s, an angle of inclination, α, is calculated for the regression line. This angle is referred to as the scaling exponent for the DFA method. It is assumed that the $F(s)$ relationship follows a power-law pattern:

$$F(s) \sim s^{\alpha}, \tag{4}$$

The indicator α characterizes the presence of positive correlations ($\alpha > 0.5$) and anti-correlations ($\alpha < 0.5$).

The values of α coincide with the value of the Hurst exponent, H. The fractal dimension of the signal, D, is related to the Hurst exponent, H, as follows: $D = 2 - H$. The calculated fractal dimension using the DFA method characterizes the averaged dynamics of a process.

2.2. The MF-DFA Algorithm

The method of multifractal detrended fluctuation analysis was proposed by Kantelhardt J.W. et al. [33–35]. MF-DFA enables calculating the multifractal spectrum and study local changes in the fractal structure.

The algorithm of multifractal detrended fluctuation analysis reduces to a sequence of the following steps:

1. The first three steps of the DFA algorithm are performed.
2. The values of the fluctuation function are determined:

$$F_q(s) = \left\{\frac{1}{N_s}\sum_{v=1}^{N_s}\left[F^2(v,s)\right]^{q/2}\right\}^{1/q}, \tag{5}$$

where q—deformation parameter.

Since for $q = 0$, equality (5) contains uncertainty, an alternative expression is used:

$$F_0(s) = exp\left\{\frac{1}{2N_s}\sum_{v=1}^{N_s}\ln\left[F^2(v,s)\right]\right\}, \quad (6)$$

3. If the series under study has fractal properties, then the fluctuation function $F(s)$ is described by a power-law dependence:

$$F_q(s) \sim s^{h(q)}, \quad (7)$$

where $h(q)$—the generalized Hurst exponent.

If the series of data in question is monofractal, then $h(q)$ in Equation (7) will take a single value $h(q) = H$. In the case of a multifractal, the index h becomes dependent on the deformation parameter q.

The multifractal set is characterized by the scaling exponent $\tau(q)$. This function shows how heterogeneous the set of points under study is. The generalized Hurst exponent is related to the function $\tau(q)$ by the ratio:

$$\tau(q) = qh(q) - 1, \quad (8)$$

The multifractal spectrum is calculated using the Legendre transform:

$$\alpha = \tau'(q);\ f(\alpha) = q(\alpha) - \tau(q), \quad (9)$$

where α—the singularity strength or the Hölder exponent.

2.3. Description of the Experimental Stand

In order to determine the feasibility of using the DF and MF-DFA algorithms for the acoustic control leak detection of valves in pipelines, experimental studies have been conducted.

The scheme of the experimental stand is shown in Figure 1.

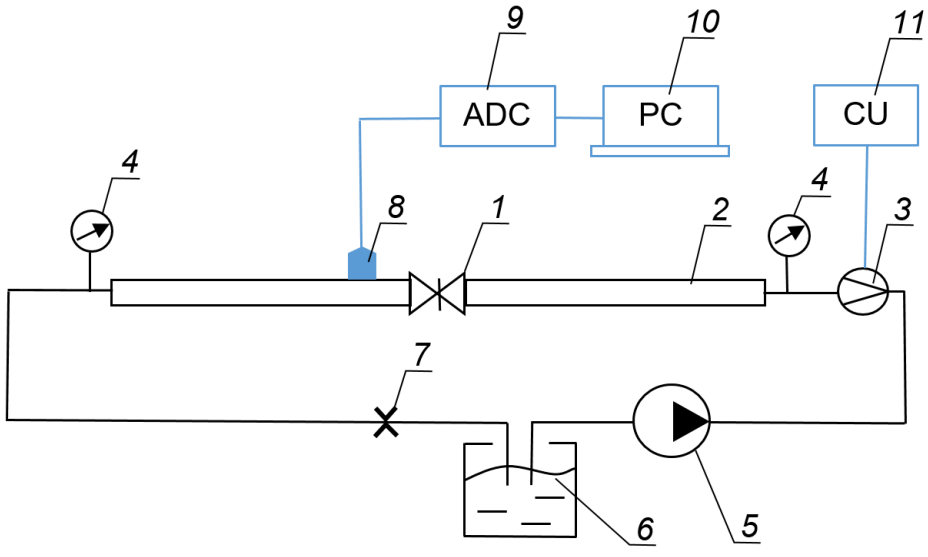

Figure 1. The experimental stand: 1—valve with a ½ inch conditional passage, 2—pipeline with ¾ inch conditional passage; 3—electromagnetic flowmeter; 4—manometer; 5—pump; 6—container with water; 7—throttle; 8—vibration acceleration sensor AP2038P-1000; 9—analog-to-digital converter Zetlab ZET 030; 10—PC with software; 11—computing unit.

Water leakage was modeled by opening a wedge gate valve 1 (with a conditional ½ inch pass) mounted on a steel pipeline 2 (with a conditional ¾ inch pass, length 2 m).

The leakage rate was controlled using an electromagnetic flowmeter 3. pressure gauges. 4. During the experiment, a pump 5 operated at a constant engine speed. To provide the necessary hydraulic resistance for the pump, a throttle 7 was used. A vibration sensor was installed next to the valve to measure vibrations in the longitudinal direction. The sensor had an axial sensitivity of 1000 mV/g and a natural frequency of 35 kHz. The analog-to-digital converter had a sampling frequency of 50 kHz.

A photo of the valve with the simulated leak is shown in Figure 2.

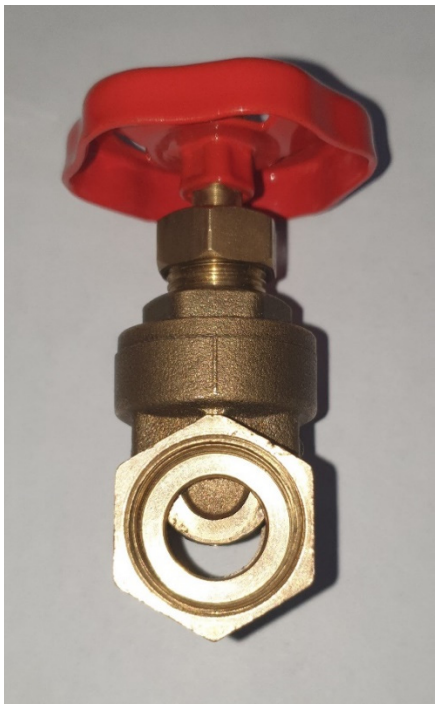

Figure 2. Photo of the wedge gate valve.

Table 1 shows the results of measuring pressure and water flow at different degrees of valve opening. The water consumption when the valve is fully open is 22.0 L per minute.

Table 1. The results of measuring the pressure and flow of water at different degrees of valve opening.

Excess Pressure at the Valve Inlet, Bar	Excess Pressure at the Outlet of the Valve, Bar	Pressure Drop on the Valve, Bar	Water Consumption, L/min	Note
1.48	1.43	0.05	22.0	valve is fully open
1.55	1.19	0.36	20.0	
1.65	0.85	0.80	16.8	
1.71	0.60	1.11	14.0	
1.79	0.24	1.55	10.5	
1.85	0	1.85	5.3	
1.97	0	1.97	0	valve is completely closed

A sample of 20 acoustic signals, each with a length of 20,000 samples, was analyzed for different degrees of opening of the gate valve. The fluctuation function was calculated on signal sections (windows), with a length s = 16 to 1024.

3. Results

3.1. The Results of the Analysis of Acoustic Signals Using the DFA-1 Method

The results of the DFA-1 signal analysis are shown in Figure 3.

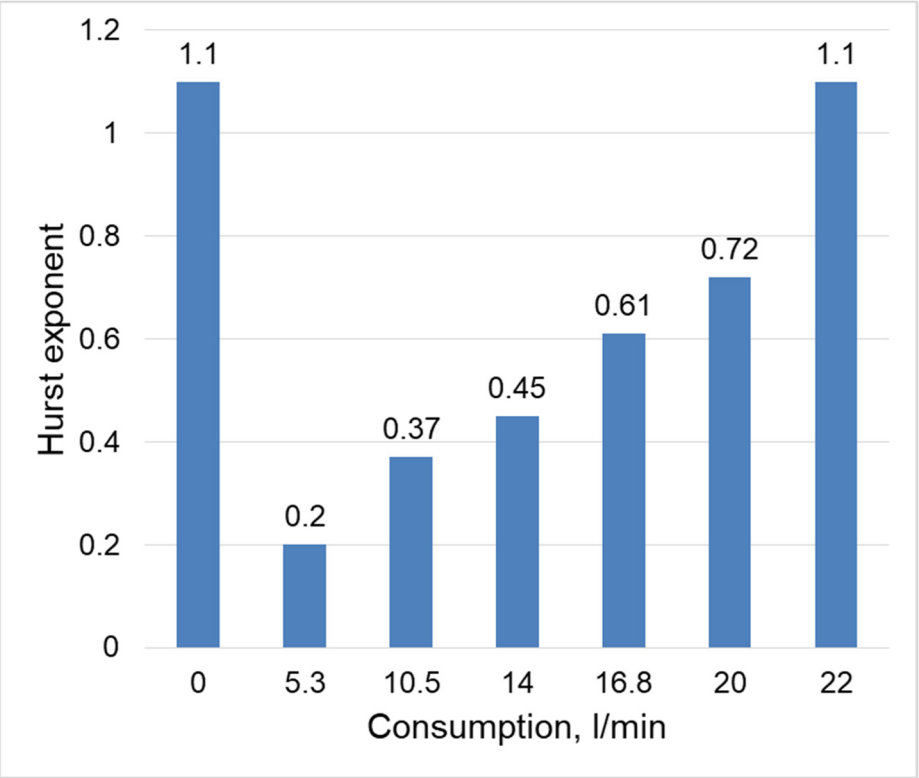

Figure 3. The results of the calculation of the Hurst exponent for acoustic signals using the DFA-1 method (median values for 20 acoustic signals).

When the valve is fully open (the consumption is 22.0 L/min) and fully closed (the consumption is 0 L/min), the Hurst exponent for acoustic signals is at a level of a deterministic signal ($H \to 1$). At low valve opening values, the acoustic signals are anticorrelated (with alternating large and small amplitudes). For these, the Hurst exponent is below the level of a probabilistic process ($H < 0.5$). An increase in leakage leads to an increase in the Hurst exponent. With high fluid consumption a positive correlation is observed between the signals ($H > 0.5$, small amplitudes often follow small amplitudes, and large amplitudes follow large amplitudes).

Figure 4 shows the power spectrum of acoustic signals obtained by median averaging of the signals.

The power spectrum of the acoustic signal of a hermetically sealed valve (black line in Figure 4) decreases uniformly on a logarithmic frequency scale. If there is a water leak, the energy in the acoustic signal will increase. For a fully open gate valve (blue line in Figure 4), the highest signal energy is observed in the low-frequency region (up to 5 kHz). With a decrease leakage consumption, a redistribution of acoustic energy from low frequencies to higher frequencies is observed (red and green lines in Figure 4).

The appearance of high-frequency fluctuations can be seen in the profiles of the acoustic signals (Figure 5), which were calculated using Equation (1).

The fluctuation profiles of the acoustic signal with the valve fully closed and fully open do not visually differ (Figure 5a,b, respectively), their Hurst exponent H is at the same level. When the valve is closed and the water flow is reduced, the fluctuation profiles become more noisy (Figure 5c,d), the Hurst exponent H decreases.

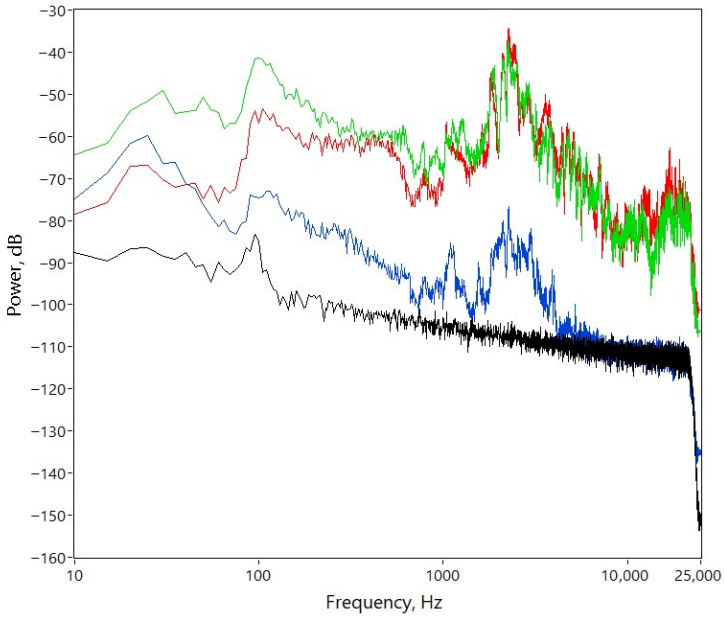

Figure 4. The power spectrum of acoustic signals obtained at different water leakage values: black—a closed valve; blue—the consumption is 22.0 L/min (open valve); green—the consumption is 16.8 L/min; red—the consumption is 5.3 L/min.

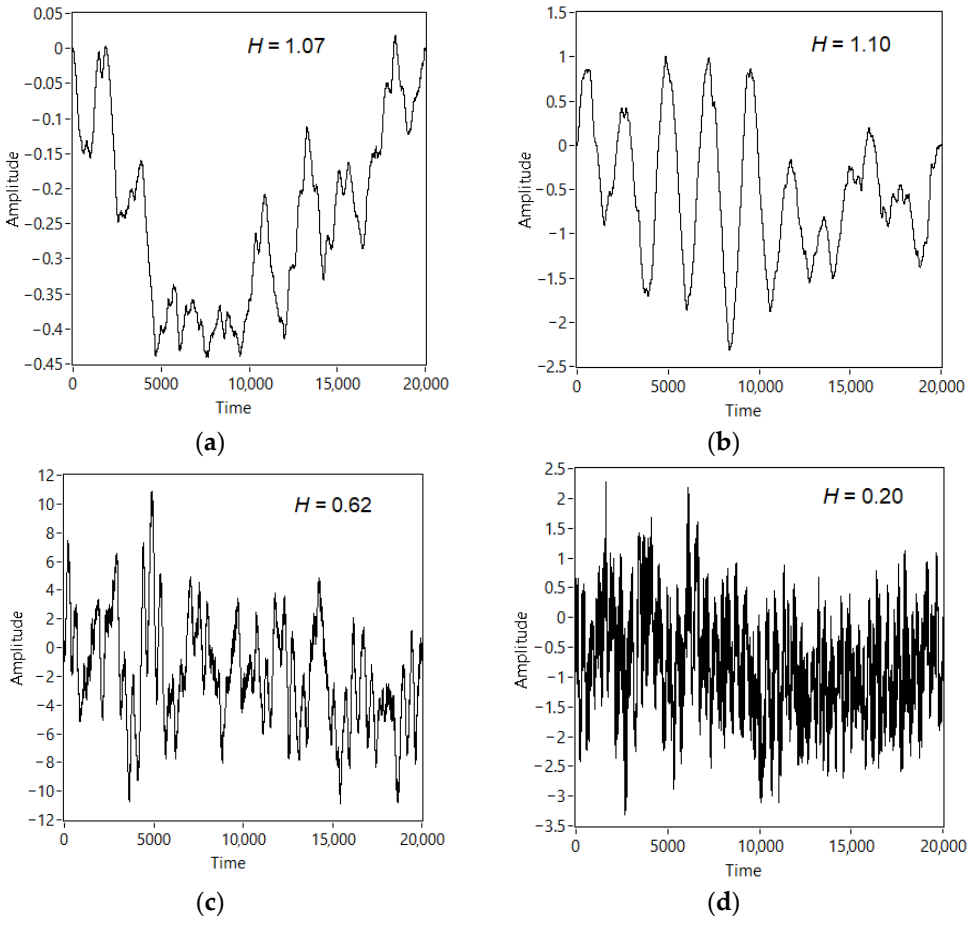

Figure 5. Fluctuation profiles of acoustic signals: (**a**) the valve is hermetically closed and the consumption is 0 L/min. (**b**) The consumption is 22.0 L/min. (**c**) The consumption is 16.8 L/min. (**d**) The consumption decreases to 5.3 L/min.

3.2. Computational Fluid Dynamics (CFD) Modeling

The results of experimental studies are consistent with numerical modeling in the software package Ansys Fluent.

During the experiments, the required number of turns of the valve handle were recorded for each value of water leakage. After removing the valve from the experimental stand, the height of the wedge lift was determined for each position of the handle. Based on these data, cross-sectional areas of the gate valves were calculated (Table 2).

Table 2. The area of the flow passage section.

Water Consumption, L/min	The Area of the Passage, mm^2	Note
22.0	176.5	valve is fully open
20.0	68.6	
16.8	43.6	
14.0	31.3	
10.5	19.2	
5.3	7.8	

The positions of the gate valve for different cross-sectional areas are shown in Figure 6.

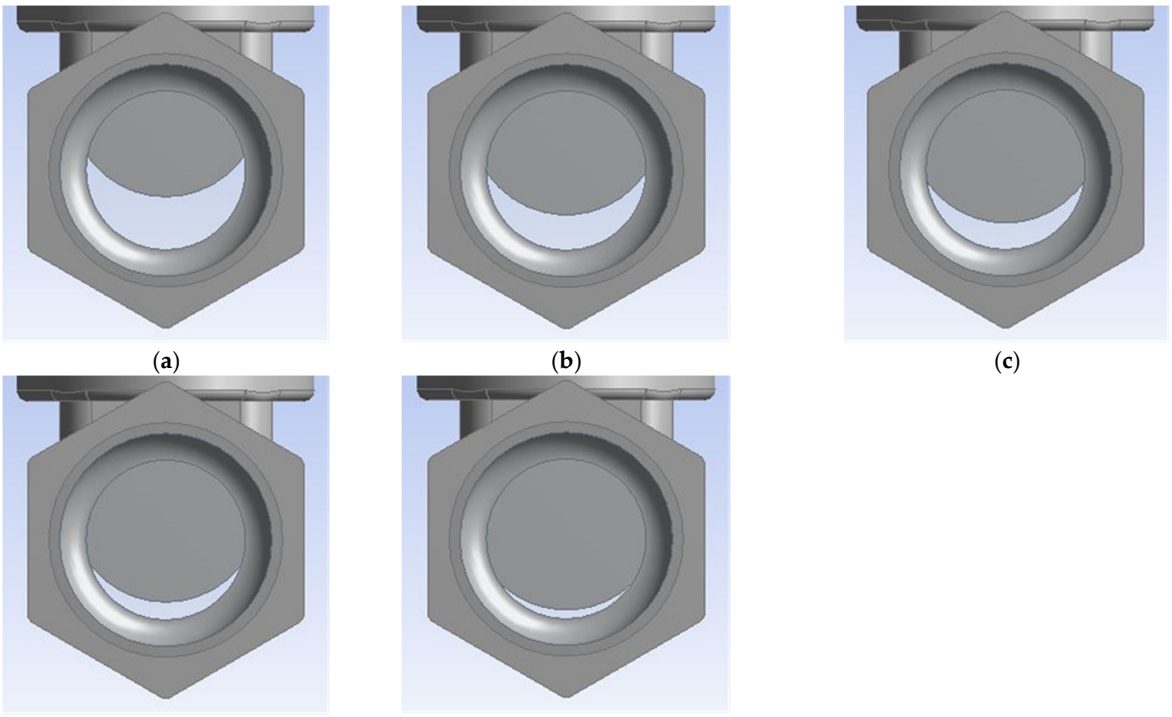

Figure 6. The positions of the gate valve at different cross-sectional areas: (**a**) 68.6 mm^2; (**b**) 43.6 mm^2; (**c**) 31.3 mm^2; (**d**) 19.2 mm^2; (**e**) 7.8 mm^2.

In Ansys Fluent, the frequencies of vortex formation in the flow with a fully open valve and different positions of the gate are calculated. For calculation k-ω SST turbulence model was used. The calculations were carried out in a non-stationary formulation of the problem, the Coupled solution algorithm with third-order discretization (Third-Order MUSCL) was used, convergence was achieved at the level of residuals 10^{-5}.

The water velocity was set at inlet to the pipe, and the pressure was set at outlet exit from the pipe. These flow parameters were obtained during a full-scale experiment and are presented in Table 3.

Table 3. Flow parameters specified in the calculations.

The Area of the Passage, mm^2	Speed at Inlet to the Pipeline, m/s	Excess Pressure at the Outlet of the Pipeline, Bar
176.5	1.17	1.43
68.6	1.06	1.19
43.6	0.89	0.85
31.3	0.75	0.60
19.2	0.56	0.24
7.8	0.28	0

Figure 7 shows the spatial distribution along the pipeline axis turbulence eddy frequencies.

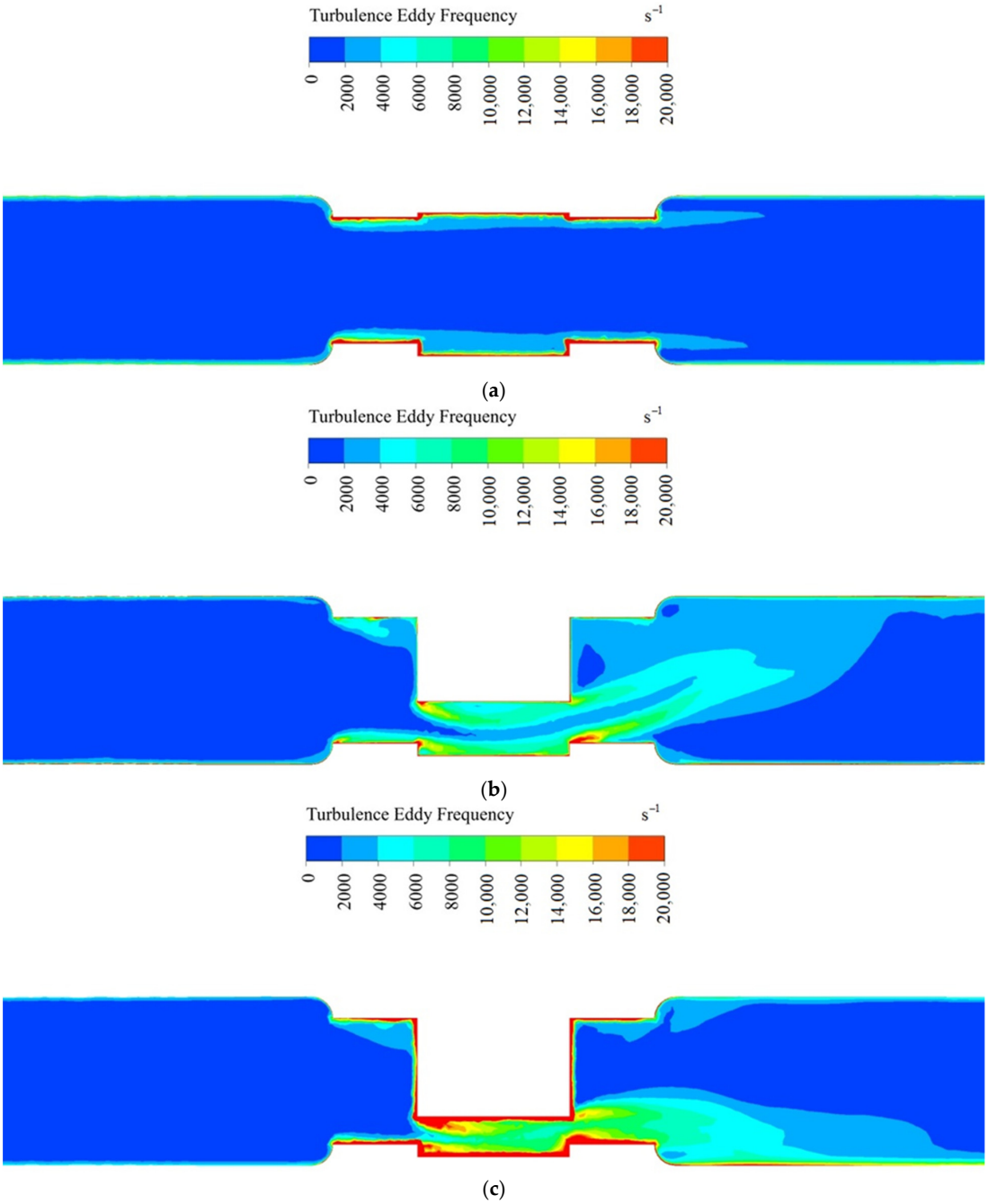

Figure 7. *Cont.*

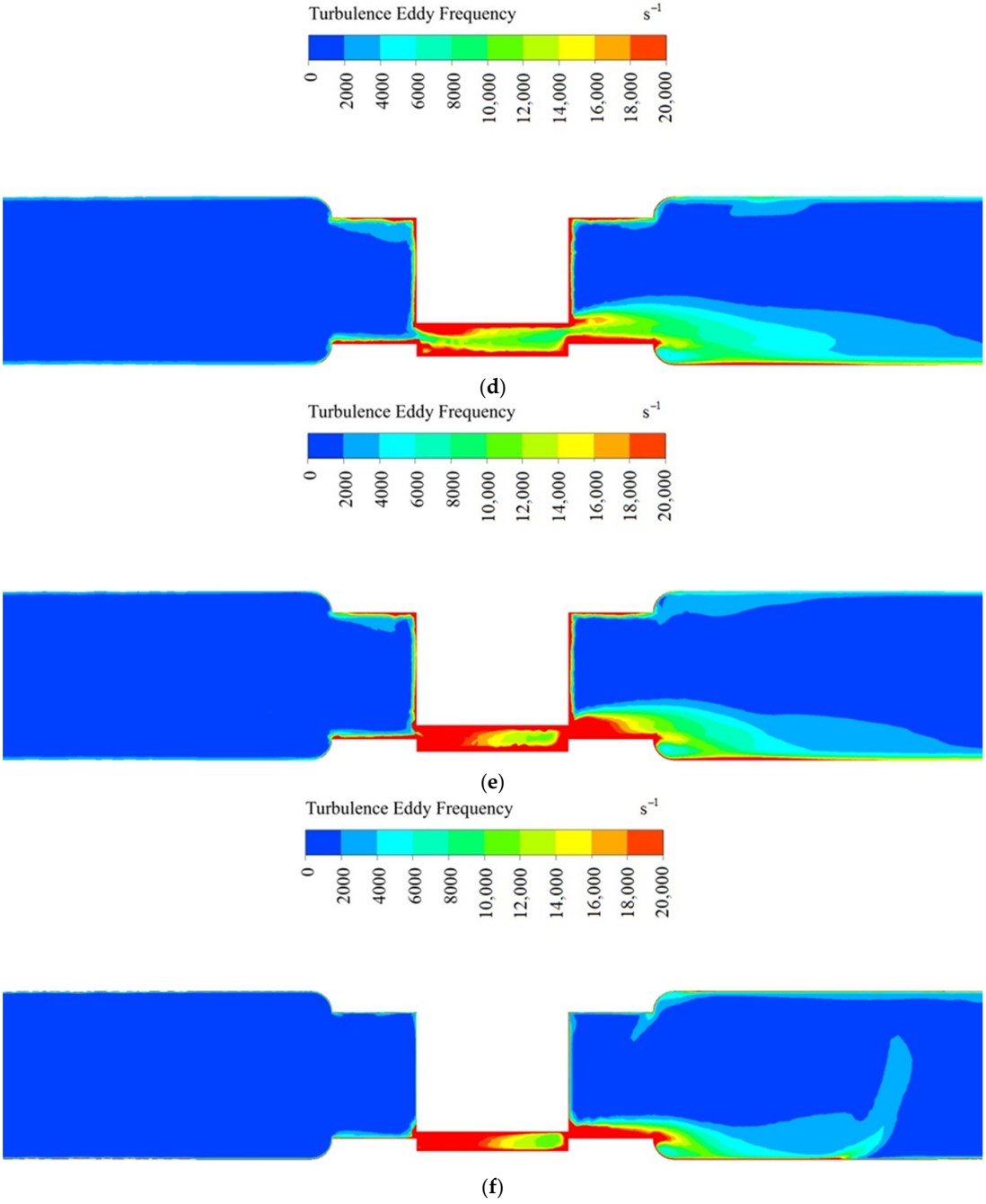

Figure 7. Spatial distribution along the pipeline axis turbulence eddy frequencies with different cross-sectional areas of the valve: (**a**) 176.5; (**b**) 68.6 mm^2; (**c**) 43.6 mm^2; (**d**) 31.3 mm^2; (**e**) 19.2 mm^2; (**f**) 7.8 mm^2.

Analyzing the data obtained as a result of numerical modeling, it can be concluded that, at low values of leakage, areas with a high turbulence eddy frequency increase. An increase in the frequency of turbulent pulsations leads to increased energy dissipation. Part of the energy from ordered processes is transferred to energy in disordered processes. The acoustic signal becomes more fragmented, and its Hurst exponent decreases.

3.3. Comparison of DFA Methods of Different Orders

Within the framework of the DFA algorithm, the standard error of approximation for the generalized model of a wandering particle is analyzed, depending on the size

of the approximated area. The order of this method is determined by the order of the approximating polynomial.

Figure 8 shows the results of calculating the Hurst exponent using DFA methods with different orders.

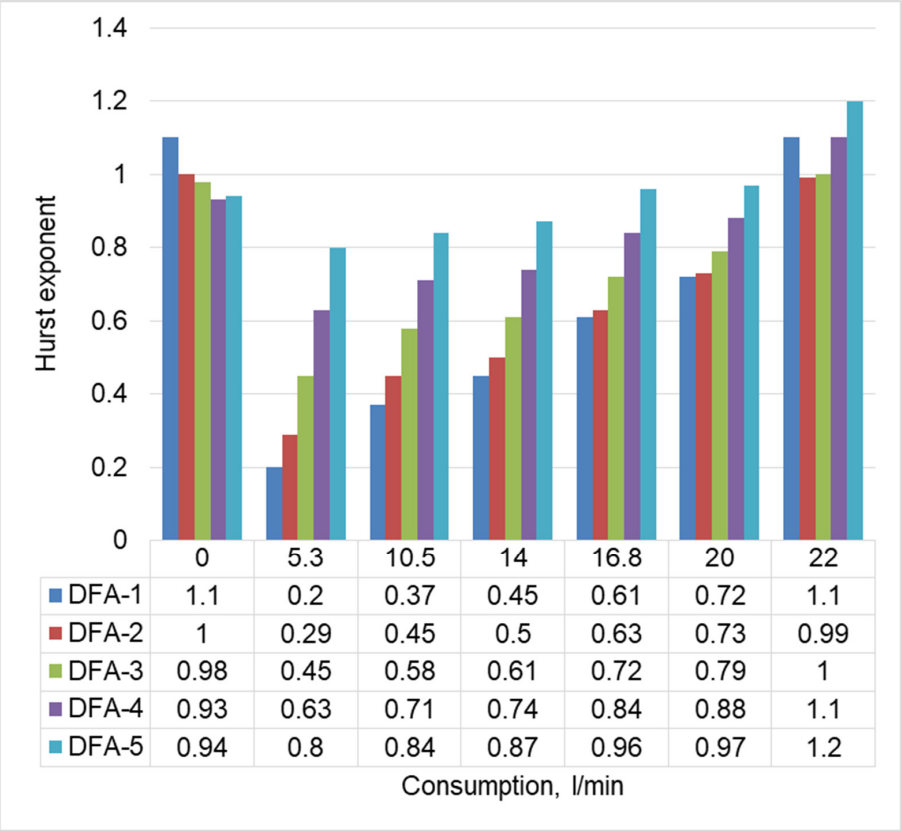

	0	5.3	10.5	14	16.8	20	22
DFA-1	1.1	0.2	0.37	0.45	0.61	0.72	1.1
DFA-2	1	0.29	0.45	0.5	0.63	0.73	0.99
DFA-3	0.98	0.45	0.58	0.61	0.72	0.79	1
DFA-4	0.93	0.63	0.71	0.74	0.84	0.88	1.1
DFA-5	0.94	0.8	0.84	0.87	0.96	0.97	1.2

Figure 8. Results of calculating the Hurst exponent of acoustic signals using DFA methods of different orders (median values for 20 acoustic signals).

It can be seen that the calculation results significantly depend on the choice of degree of approximating polynomial, and the use of high-order polynomials leads to increase in values of Hurst exponent for small leaks, reducing sensitivity of leak detection. Therefore, it is recommended to use DFA-1 for monitoring the tightness of gates.

3.4. The Results of the Analysis of Acoustic Signals Using the MF-DFA Method

In the MF-DFA calculation, deformation parameter, q, was set in the range $[-10, 10]$.

Figure 9 shows examples of the multifractal spectrum of acoustic signals. The spectra have different widths, and significant asymmetry is observed in them.

The shape of the multifractal spectrum of with a sealed and fully opened valve differs from the typical parabolic form found in multifractal objects. Similar spectra were obtained in article [36].

For quantitative analysis of the multifractal spectrum, the width W and the long tail type ΔS were calculated [35]:

$$W = \alpha_{max} - \alpha_{min}, \tag{10}$$

$$\Delta S = R - L, \tag{11}$$

$$R = \alpha_{max} - \alpha_0, \tag{12}$$

$$L = \alpha_0 - \alpha_{min} \tag{13}$$

The width of the multifractal spectrum determines the range of Hurst exponent present in the signals and indicates the degree of multifractality.

The results of calculating the width of the multifractal spectrum are shown in Figure 10. It demonstrates that, with a decrease in water leakage, the width of the spectrum increases, and variations in the scale-invariant structure of signals increase. This is due to an increased energy dissipation in turbulent flow and an increased degree of disorder in oscillatory processes at low water flow rates. For a hermetically sealed valve, the acoustic signal structure is close to being monofractal ($W \to 0$).

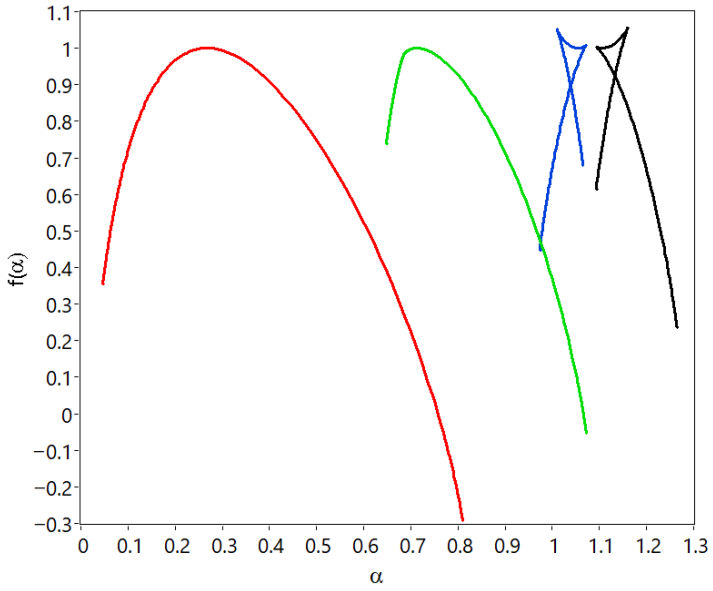

Figure 9. The multifractal spectrum of acoustic signals for different leakage rates: black line—22.0 L/min; green line—16.8 L/min; red line—5.3 L/min; blue line—0 L/min.

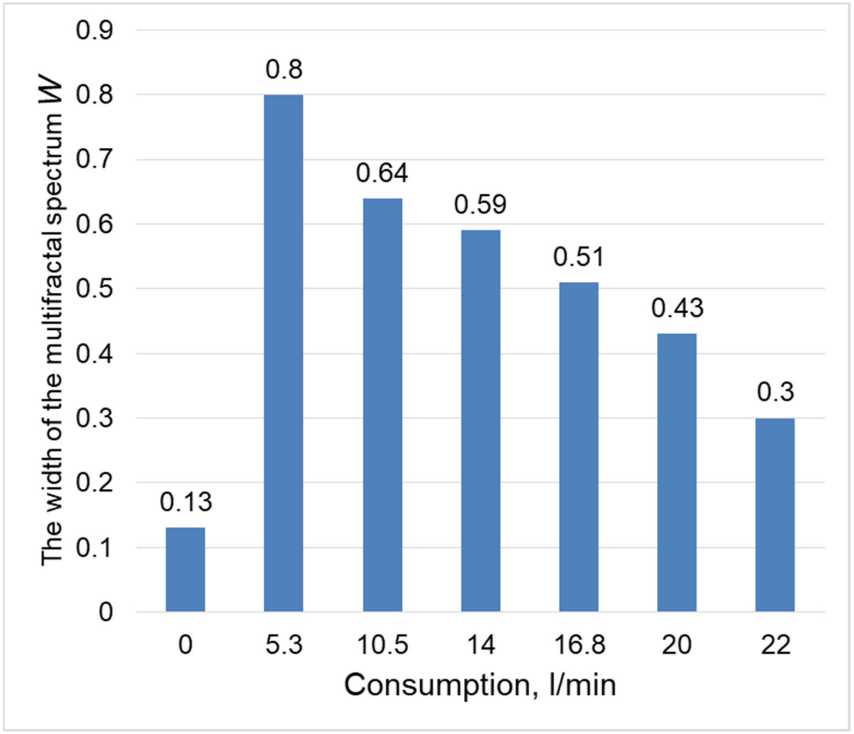

Figure 10. The width of the multifractal spectrum (median values for 20 acoustic signals).

Figure 11 shows the parameter values ΔS.

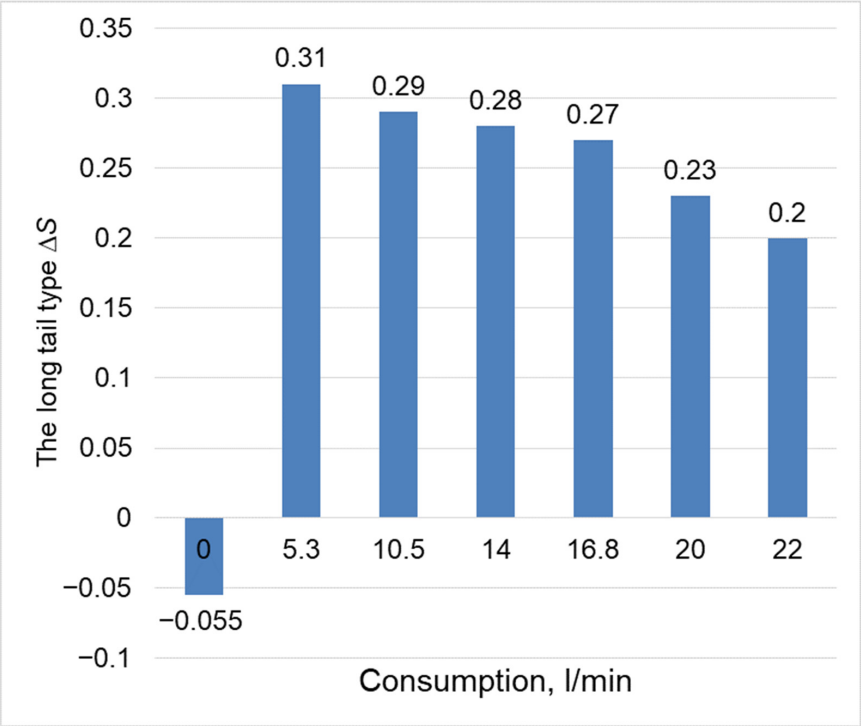

Figure 11. Long tail type (median values for 20 acoustic signals).

If there is a leak $\Delta S > 0$ ($R > L$). This means that the multifractal spectrum has long right tails. Such a multifractal structure is not sensitive to local fluctuations with large magnitudes. The main contribution is made by small noise-like fluctuations [35]. This is due to the presence of small vortices in the water flow, which occur with a high frequency.

4. Conclusions

When the tightness of the gate valve is violated, the fractal characteristics of acoustic signals change. Analysis of acoustic signals using the DFA and MF-DFA techniques enables determining the size of water leakage through a leaky gate valve.

The Hurst exponent of acoustic signals for a sealed valve is at the level of deterministic signal ($H \to 1$), and the width of the multifractal spectrum is close to that of the monofractal process. ($W \to 0$).

With the appearance of a leak, turbulent flow pulsations occur. With small leak sizes, the acoustic signals are anticorrelated and have a high degree of multifractality (for example, with a leak of 5.3 L/min $H = 0.2$, $W = 0.8$). This is due to an increase in the turbulence eddy frequency in the water flow and increased energy dissipation. Increased leakage leads to an increase in the Hurst exponent and a decrease in the width of the multifractal spectrum (with a leakage of 22 L/min $H = 1.1$, $W = 0.3$). The main contribution to the multifractal structure of leakage signals is made by small, noise-like fluctuations.

The results of calculating the Hurst exponent using the DFA method depend on the choice of degree of approximating polynomial. To control the tightness of the valve, it is advisable to use linear approximation.

Author Contributions: Conceptualization, A.Z. and S.Z.; software A.Z.; investigation, S.Z., E.I., I.K. and R.A.; validation, Y.V.; writing—original draft preparation, S.Z. and E.I.; writing—review and editing, A.Z.; data curation, I.K. and R.A. All authors have read and agreed to the published version of the manuscript.

Funding: This research was funded by the Russian Science Foundation grant No. 22-79-10045, https://rscf.ru/en/project/22-79-10045/ (accessed date 10 April 2024).

Data Availability Statement: The data presented in this study are available on request from the corresponding author.

Conflicts of Interest: The authors declare no conflicts of interest.

References

1. Kaihong, X. Research on the Application of Automatic Control System in Mechanical Engineering. *Adv. Comput. Sci. Res.* **2018**, *78*, 79–82. [CrossRef]
2. Xu, C.; Han, G.; Gong, P.; Chen, G.; Zhang, L. Quantification of Internal Air Leakage in Ball Valve using Acoustic Emission Signals. *E J. Nondestruct. Test.* **2016**, *21*, 19328. Available online: https://www.ndt.net/?id=19328 (accessed on 10 April 2024).
3. Ding, Z.; Shang, Q.; Li, J.; Fang, Y.; Liu, Y. The Diagnosis of Internal Leakage of Control Valve Based on the Grey Correlation Analysis Method. *Sens. Transducers* **2014**, *175*, 44–50.
4. Hunaidi, O.; Chu, W.T. Acoustical characteristics of leak signals in plastic water distribution pipes. *Appl. Acoust.* **1999**, *58*, 235–254. [CrossRef]
5. Meland, E.; Henriksen, V.; Hennie, E.; Rasmussen, M. Spectrum analysis of internally leaking shut-down valves. *Measurement* **2011**, *44*, 1059–1072. [CrossRef]
6. Kaewwaewnoi, W.; Prateepasen, A.; Kaewtrakulpong, P. Investigation of the relationship between internal fluid leakage through a valve and the acoustic emission generated from the leakage. *Measurement* **2010**, *43*, 274–282. [CrossRef]
7. Prateepasen, A.; Kaewwaewnoi, W.; Kaewtrakulpong, P. Smart portable noninvasive instrument for detection of internal air leakage of a valve using acoustic emission signals. *Measurement* **2011**, *44*, 378–384. [CrossRef]
8. Meland, E.; Thornhill, N.F.; Lunde, E.; Rasmussen, M. Quantification of Valve Leakage Rates. *AIChE J.* **2012**, *58*, 1181–1193. [CrossRef]
9. Ye, G.Y.; Xu, K.J.; Wu, W.K. Multivariable modeling of valve inner leakage acoustic emission signal based on Gaussian process. *Mech. Syst. Signal Process.* **2020**, *140*, 106675. [CrossRef]
10. Ye, G.Y.; Xu, K.J.; Wu, W.K. Standard deviation based acoustic emission signal analysis for detecting valve internal leakage. *Sens. Actuator A Phys.* **2018**, *283*, 340–347. [CrossRef]
11. Xiao, R.; Hu, Q.; Li, J. Leak detection of gas pipelines using acoustic signals based on wavelet transform and Support Vector Machine. *Meas. J. Inetrnational Meas. Confed.* **2019**, *146*, 479–489. [CrossRef]
12. Heo, G.; Lee, S.K. Internal leakage detection for feed water heaters in power plants using neural networks. *Expert Syst. Appl.* **2012**, *39*, 5078–5086. [CrossRef]
13. Zhu, S.B.; Li, Z.L.; Zhang, S.M.; Zhang, H.F. Deep belief network-based internal valve leakage rate prediction approach. *Measurement* **2019**, *133*, 182–192. [CrossRef]
14. Datta, D.; Sathish, S. Application of fractals to detect breast cancer. *J. Phys. Conf. Ser.* **2019**, *1377*, 012030. [CrossRef]
15. Hart, M.G.; Romero-Garcia, R.; Price, S.J.; Suckling, J. Global effects of focal brain tumors on functional complexity and 461 network robustness: A prospective cohort study. *Clin. Neurosurg.* **2019**, *84*, 1201–1213. [CrossRef] [PubMed]
16. Dona, O.; Hall, G.B.; Noseworthy, M.D. Temporal fractal analysis of the rs-BOLD signal identifies brain abnormalities in autism spectrum disorder. *PLoS ONE* **2017**, *12*, e0190081. [CrossRef] [PubMed]
17. Jiang, Z.-Q.; Xie, W.-J.; Zhou, W.-X.; Sornette, D. Multifractal Analysis of Financial Markets: A Review. *Rep. Prog. Phys.* **2019**, *82*, 125901. [CrossRef] [PubMed]
18. Chandrasekaran, S.; Poomalai, S.; Saminathan, B.; Suthanthiravel, S.; Sundaram, K.; Hakkim, F.F.A. An investigation on the relationship between the hurst exponent and the predictability of a rainfall time series. *Meteorol. Appl.* **2019**, *26*, 511–519. [CrossRef]
19. Duan, Q.; An, J.; Mao, H.; Liang, D.; Li, H.; Wang, S.; Huang, C. Review about the Application of Fractal Theory in the Research of Packaging Materials. *Materials* **2021**, *14*, 860. [CrossRef]
20. Jeldres, R.I.; Fawell, P.D.; Florio, B.J. Population Balance Modelling to Describe the Particle Aggregation Process: A review. *Powder Technol.* **2018**, *326*, 190–207. [CrossRef]
21. Babanin, O.; Bulba, V. Designing the technology of express diagnostics of electric train's traction drive by means of fractal analysis. *East. Eur. J. Enterp. Technol* **2016**, *4*, 45–54. [CrossRef]
22. Li, Q.; Liang, S.Y. Degradation trend prognostics for rolling bearing using improved R/S statistic model and fractional brownian motion approach. *IEEE Access* **2017**, *6*, 21103–21114. [CrossRef]
23. Dimri, V.P.; Ganguli, S.S. Fractal Theory and Its Implication for Acquisition, Processing and Interpretation (API) of Geophysical Investigation: A Review. *J. Geol. Soc. India* **2019**, *93*, 142–152. [CrossRef]
24. Tang, S.W.; He, Q.; Xiao, S.Y.; Huang, X.Q.; Zhou, L. Fractal Plasmonic Metamaterials: Physics and Applications. *Nanotechnol. Rev.* **2015**, *4*, 277–288. [CrossRef]
25. He, J.; Li, M. Space–Time Variations in the Long-Range Dependence of Sea Surface Chlorophyll in the East China Sea and the South China Sea. *Fractal Fract.* **2024**, *8*, 102. [CrossRef]

26. Strait, B.J.; Dewey, T.G. Multifractals and decoded walks: Applications to protein sequence correlations. *Phys. Rev. E* **1995**, *52*, 6588–6592. [CrossRef]
27. Glazier, J.A.; Raghavachari, S.; Berthelsen, C.L.; Skolnick, M.H. Reconstructing phylogeny from the multifractal spectrum of mitochondrial DNA. *Phys. Rev. E* **1995**, *51*, 2665–2668. [CrossRef]
28. Hentschel, H.G.E. Stochastic multifractality and universal scaling distributions. *Phys. Rev. E* **1994**, *50*, 243–261. [CrossRef]
29. Wiklund, K.O.; Elgin, J.N. Multifractality of the Lorenz system. *Phys. Rev. E* **1996**, *54*, 1111–1119. [CrossRef]
30. Pavlov, A.N.; Ebeling, W.; Molgedey, L.; Ziganshin, A.R.; Anishchenko, V.S. Scaling features of texts, images and time series. *Phys. A* **2001**, *300*, 310–324. [CrossRef]
31. Pavlov, A.N.; Sosnovtseva, O.V.; Ziganshin, A.R.; Holstein-Rathlou, N.H.; Mosekilde, E. Multiscality in the dynamics of coupled chaotic systems. *Phys. A* **2002**, *316*, 233–249. [CrossRef]
32. Peng, C.K.; Buldyrev, S.V.; Havlin, S.; Simons, M.; Stanley, H.E.; Goldberger, A.L. Mosaic Organization of DNA Nucleotides. *Phys. Rev. E* **1994**, *49*, 1685–1689. [CrossRef] [PubMed]
33. Kantelhardt, J.W.; Zschiegner, S.A.; Koscielny-Bunde, E.; Havlin, S.; Bunde, A.; Stanley, H.E. Multifractal Detrended Fluctuation Analysis of Nonstationary Time Series. *Phys. A Stat. Mech. Its Appl.* **2002**, *316*, 87–114. [CrossRef]
34. Espen, A.F. Ihlen. Introduction to Multifractal Detrended Fluctuation Analysis in Matlab. *Front. Physiol.* **2012**, *3*, 141. [CrossRef]
35. Zhang, X.; Liu, H.; Zhao, Y.; Zhang, X. Multifractal detrended fluctuation analysis on air traffic flow time series: A single airport case. *Phys. A Stat. Mech. Its Appl.* **2019**, *531*, 121790. [CrossRef]
36. Zagretdinov, A.; Ziganshin, S.; Izmailova, E.; Vankov, Y.; Klyukin, I.; Alexandrov, R. Detection of Pipeline Leaks Using Fractal Analysis of Acoustic Signals. *Fractal Fract.* **2024**, *8*, 213. [CrossRef]